

Macromolecular Dynamics in Solid Poly(ethylene terephthalate): ^1H and ^{13}C Solid-State NMR[†]

Alan D. English

Central Research and Development Department, E. I. du Pont de Nemours and Co.,
Wilmington, Delaware 19898. Received December 14, 1983

ABSTRACT: Results of various ^1H and ^{13}C solid-state NMR experiments are reported for a variety of poly(ethylene terephthalate) samples. These results indicate that four separate motional processes can be distinguished: a very rapid reorientation of polymer segments in which the amplitude of the motion grows as a function of temperature, a slower specific motion of the benzene rings (perhaps flipping) that correlates with the β relaxation, an even slower motion that is unique to the methylene groups (perhaps *trans* \leftrightarrow *gauche* isomerization) that correlates with the α relaxation, and an almost effectively isotropic reorientation of some amorphous polymer segments whose population is temperature dependent. These results also indicate that these particular NMR experiments are sensitive to the crystallinity of the polymer but do not differentiate powdered, fiber, or film samples of comparable crystallinity. A simple formalism for describing temperature-dependent growth of spatial averaging and its influence upon dipolar-dominated NMR phenomena (line width, $T_{1\rho}$, and T_1) is presented.

Introduction

A brief summary of previous experimental results and conclusions as to the structure and dynamics of poly(ethylene terephthalate) (PET) will be useful in analyzing our results. We concentrate primarily on NMR results but also draw on dielectric and mechanical relaxation data where necessary. PET can be prepared in a range of crystallinities from nearly amorphous to 50–60% crystalline; the amorphous glass transition temperature is $\sim 67^\circ\text{C}$ and the glass transition in semicrystalline samples is $\sim 80^\circ\text{C}$.¹ There are two major viscoelastic relaxations in PET below the melting point (260°C). The α relaxation occurs in the range 90 – 135°C at 100 Hz , depending upon crystallinity and orientation (see Figure 1) and is thought to involve micro-Brownian motion in the amorphous part of the polymer; the effective activation energy is 100 – 200 kcal/mol . The β relaxation occurs at -50°C at 100 Hz and is thought to correspond to limited motions of all portions of the polymer in both crystalline and amorphous regions; the effective activation energy is 13 – 17 kcal/mol . The frequency and temperature dependences of the α and β relaxations are shown in Figure 1.¹

The largest number of NMR investigations of PET dynamics and morphology have been reported by Ward² and collaborators and, more recently, Eichhoff and Zachmann⁴ have reinvestigated the subject. Ward's initial results did not show any structure in the NMR spectrum from 20 to 465 K , and the second moment (M_2) of the rigid lattice NMR line shape was much larger than that calculated from the then known crystal structure;⁵ T_1 measurements indicated an "activation energy" of 2 kcal/mol . The difference between the calculated M_2 (second moment of the ^1H NMR line shape) of a PET crystal and the values of M_2 obtained for semicrystalline samples was attributed to a closer intermolecular approach of methylene segments in amorphous regions than in crystalline regions. Furthermore, the process responsible for the observed T_1 behavior was argued to be the β relaxation; the low value calculated from the activation energy was rationalized by the usual distribution of correlation times arguments.³ Later results^{2c,d} on selectively deuterated PET (deuterated glycol residue or deuterated terephthalic acid residue) and other fully protonated polyesters with longer glycol residues led to the observation of mobile (narrow line) and immobile (broad line) fractions in PET. The mobile fraction appeared around 110°C and was composed of

contributions from both methylene and aromatic protons; the broad line was observed to contain contributions from rigid aromatic protons and motionally hindered aliphatic protons. The T_1 's of amorphous and semicrystalline fully protonated samples were observed to be the same and, therefore, the motion of the methylene groups was thought to be the same in the amorphous and crystalline regions. The fraction of the sample observed to be mobile increased with temperature over the range 110 – 170°C , corresponding to 0% to 50 – 100% of the sample over this temperature range. The picture of PET macromolecular dynamics derived from these results has been repeated many times in the literature. Subsequent results by Ward, Eichhoff, and Zachmann and ourselves show that this picture is subject to some reinterpretation and modification.

Eichhoff and Zachmann⁴ made several contributions regarding the interpretation of NMR experiments on PET. They reinvestigated Ward's report that the second moment of the NMR line shape for semicrystalline PET was larger than that calculated for crystalline PET. They found that the second moment for semicrystalline PET is smaller than their value (based on then new electron diffraction data) calculated for a completely crystalline sample. In addition, they extrapolated their experimental results to predict the experimental M_2 for a completely crystalline sample and found this value to be in close agreement with their calculation of M_2 for a PET crystal ($13.1 \pm 1.2\text{ G}^2$ calculated, 12.6 G^2 extrapolated experimental). This finding obviated Ward's postulate about the close contact of methylene groups in the amorphous region. These authors also discussed the origin of the broad and narrow lines in the NMR spectra. The NMR data defined the relative amounts of mobile (narrow line) and immobile (broad line) components as a function of temperature and also the contribution of methylene and aromatic groups to each component. Their data indicated the following: (1) Methylene group reorientation begins below T_g . (2) At the onset of T_g , all methylene groups are reorienting and the aromatic groups are rigid. (3) At higher temperatures the aromatic groups in the noncrystalline regions begin to reorient; however, the aromatic groups do not contribute to the mobile fraction (narrow line). (4) At even higher temperatures the aromatic groups in the noncrystalline regions begin to undergo "micro-Brownian" motion and give rise to a narrow component. The broad component is still due to methylene groups undergoing hindered rotations and rigid aromatic groups. (5) The fraction of mobile species (narrow line) grows from $\sim 10\%$ at 120°C

[†]Contribution No. 3426.

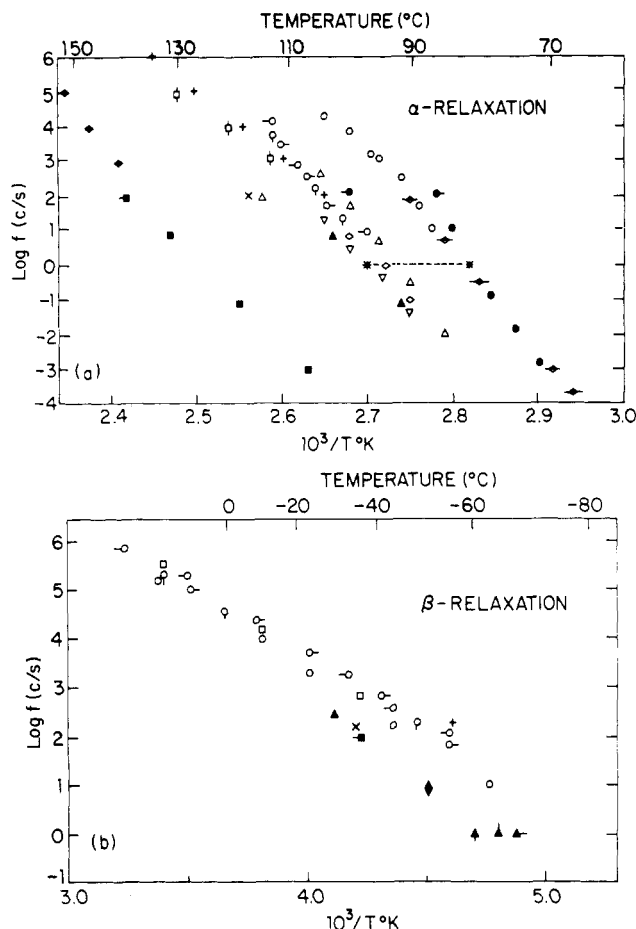


Figure 1. Relaxation map of the α (upper) and β (lower) relaxations in poly(ethylene terephthalate). Open symbols are dielectric relaxation results, and closed symbols are mechanical relaxation results. The values for the α relaxation fall into three groups, where the highest frequency value at constant temperature is for amorphous polymer, the intermediate value is for unoriented crystalline polymer, and the lowest value is for oriented crystalline polymer (see ref 1 for experimental details). Reprinted with permission from ref 1. Copyright 1967 John Wiley and Sons Ltd.

to ~30–40% at 200 °C. These conclusions are derived from wide-line ^1H NMR spectra of fully protonated PET that are distorted by field modulation. Our results, which are not complicated by field modulation, indicate that points 2–5 require clarification or modification. The results of these authors were combined with independent measurements (X-ray, dilatometry) of amorphous content to develop a three-phase model of PET—crystalline, rigid noncrystalline, and amorphous. The quantitative development of this model is predicated on the assumption that the measurement of the relative amount of mobile fraction has been accurately determined and is far too large to be explained as low molecular weight polymer or oligomers.

We present here the results of a large number of ^1H and ^{13}C solid-state NMR experiments on PET. These experiments have been carried out on semicrystalline powders (both fully protonated and partially deuterated), amorphous and semicrystalline fibers, and amorphous and semicrystalline films. These results indicate that different types of motion can be assigned to different portions of the polymer. Recognition that both spatial and temporal averaging are temperature dependent is essential to a proper interpretation of NMR observations, vis-à-vis macromolecular dynamics.

Experimental Section

^1H NMR spectra were obtained at a static field strength of 2.1 T with a Bruker SXP 4-100 NMR spectrometer. Dipolar line

widths are reported as full width at half-maximum from spectra acquired via Fourier transformation of time-domain data acquired with radio-frequency pulses of length 1 μs and repetition rates greater than 3 times the spin-lattice relaxation time. Spin-lattice relaxation times in the rotating frame were measured in the conventional manner,⁶ and the radio-frequency field strength was calibrated with NH_4Br .⁷

^{13}C NMR spectra were obtained at field strengths of both 2.1 and 7.0 T with a Bruker SXP 4-100 and a Bruker CXP 300 NMR spectrometer. ^{13}C NMR spectra were obtained with a combination of cross-polarization, spin-temperature alternation, dipolar decoupling, and magic angle spinning as dictated by the experiment. Static ^{13}C spectra were acquired with a cross-polarization time of 5 ms and radio-frequency field strengths of $\gamma(H_1) = 80$ kHz for cross-polarization and dipolar decoupling. Magic angle spinning spectra were acquired at a radio-frequency field strength of 64 kHz, 5-ms cross-polarization time, and spinning rates in the range 1–5 kHz; the magic angle varied as a function of spinning rate and was adjusted via observation of the rotational echoes of KBr that had been mixed with the PET following the method of Maciel.¹¹

PET samples used included amorphous and semicrystalline film and fiber and powdered semicrystalline partially deuterated specimens. Both films were unoriented and were either amorphous (~1% crystalline) or semicrystalline (~45% crystalline). Both yarns were "oriented" and were either amorphous (~4% crystalline) or semicrystalline (49% crystalline). Semicrystalline PET with deuterated terephthalic groups was prepared from deuterated terephthalic acid and ethylene glycol by standard melt condensation methods and was found to be ~55% crystalline. Semicrystalline PET with deuterated methylene groups was prepared from deuterated ethylene glycol and dimethyl terephthalate and was found to be ~60% crystalline. Fully protonated polymers were made via both of the two methods and were found to have the same crystallinity as the respective deuterated polymers. The approximate crystallinity values given here were determined by dilatometry⁸ and represent the as-polymerized crystallinity (not annealed). The molecular weight as determined by inherent viscosity was $M_n \approx 23\,000$ for the fully protonated polymer and $M_n \approx 20\,000$ for the partially deuterated polymers. All samples were sparged with N_2 and stored in capped NMR tubes in an effort to retard degradation at high temperatures.

Results

Proton NMR: Powdered Semicrystalline Poly(ethylene terephthalate). ^1H FTNMR spectra as a function of temperature were recorded for the semicrystalline powdered samples from ~170 to +230 °C. In each case there appeared to be at least two components in the line shape, one of which was narrower and accounted for a small portion of the specimen at most temperatures and the other of which was a broad featureless line. The broad portion of the line shape corresponds to a relatively less mobile species. The temperature dependence of the line width (full width at half-maximum) of the relatively immobile fraction of the line shape for powdered semicrystalline PET is shown in Figure 2. Figure 2 illustrates a number of points for powdered semicrystalline poly(ethylene terephthalate) that may be summarized as follows:

1. The line width (or M_2) observed at the lowest temperature indicates that the rigid lattice or slow-motion limit is reached by ~170 °C.

2. The line widths observed for both fully protonated polymers are essentially identical. The line width of the fully protonated polymer is near the simple average of the separate aliphatic and aromatic line widths since there is an equal number of protons in each site. This simple averaging is consistent with a structure in which the preferred packing does not prefer close approach of aromatic and aliphatic protons.^{3,4} In addition to the relatively broad line, a narrow line is also initially observed in each case near -10 ± 10 °C. The relative intensity of the narrow

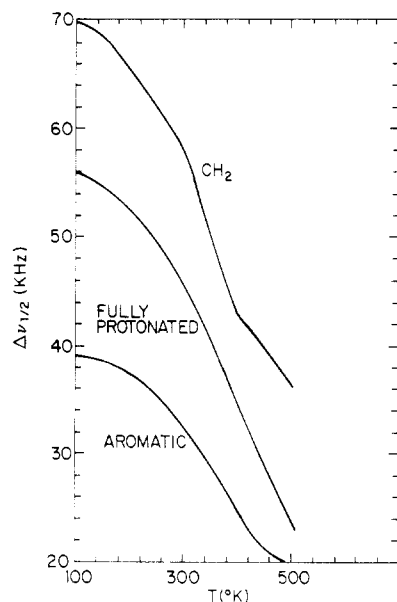


Figure 2. Proton NMR line width as a function of temperature for partially deuterated poly(ethylene terephthalate). The curve labeled "CH₂" is for the polymer made from deuterated terephthalic acid, the curve labeled "aromatic" is for the polymer made from deuterated ethylene glycol, and the curve labeled "fully protonated" is for the polymer synthesized from dimethyl terephthalate and ethylene glycol.

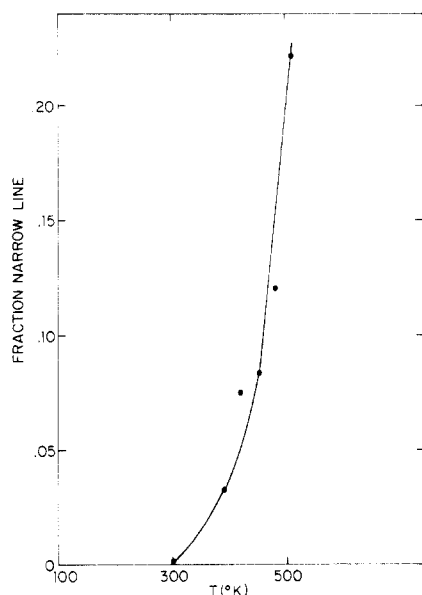


Figure 3. Fraction of the total proton free induction decay of poly(ethylene terephthalate) that appears as the narrower line as a function of temperature.

component increases with temperature and is illustrated in Figure 3 for the fully protonated polymer. The relative intensities of these two components are calculated from the free induction decay. The size of both the Gaussian and exponential contributions to the free induction decay is calculated from 45 points acquired in the 100 μ s following a $\pi/2$ radio-frequency pulse; the Gaussian contribution is extracted from the short-time behavior, which is linear in a semilogarithmic plot vs. t^2 , and the exponential contribution is extracted from the long-time behavior, which is linear in a semilogarithmic plot vs. t .⁹ Both contributions were corrected for finite pulse width and receiver blanking (4 μ s) by extrapolating back in time to the middle of the radio-frequency pulse. The line width of the narrow component of the line shape was ~ 15 kHz

Table I
¹H NMR Line Width of the Narrow Component of the Poly(ethylene terephthalate) Line Shape

T , °C	line width, kHz
147	14.0
177	8.5
207	4.5
237	2.8

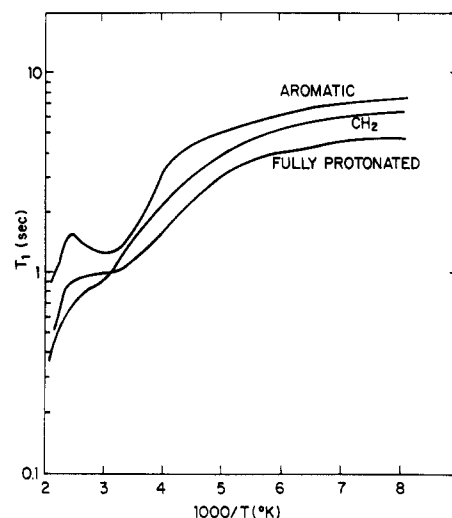


Figure 4. Proton spin-lattice relaxation time of powdered semicrystalline poly(ethylene terephthalate) at a resonant frequency of 90 MHz. Broad component of line shape only.

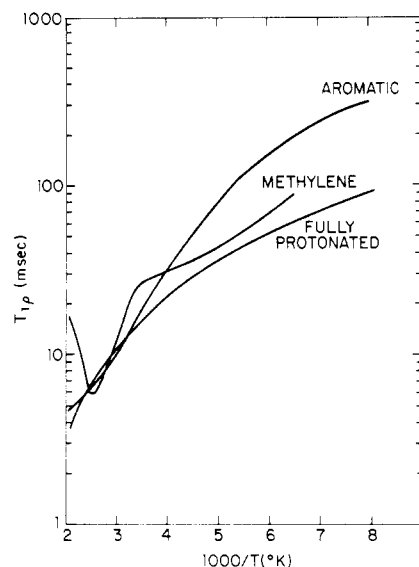


Figure 5. Proton spin-lattice relaxation time in the rotating frame ($\gamma(H_1) = 50$ kHz) of powdered semicrystalline poly(ethylene terephthalate).

at room temperature and decreased to ~ 2.8 kHz at 235 °C (see Table I).

Spin-lattice relaxation times in the static field (T_1) and in the rotating frame ($T_{1\rho}$) were obtained as a function of temperature and are illustrated in Figures 4 and 5, respectively. Relaxation times reported are associated with the broad feature of the line shape. The magnetization decay was observed to be singly exponential in the T_1 measurements, and the weak temperature dependence of T_1 below ca. 50 °C may reflect contributions to the relaxation from paramagnetic oxygen gas not removed by N₂ sparging. The reported $T_{1\rho}$ values are the long-time limiting slope, which ignores an apparent 10–30% component that relaxes more rapidly.

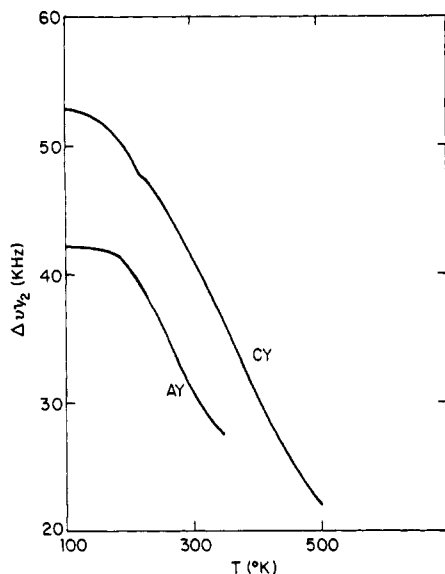


Figure 6. Proton NMR line width as a function of temperature for amorphous yarn (AY) and semicrystalline yarn (CY) of poly(ethylene terephthalate).

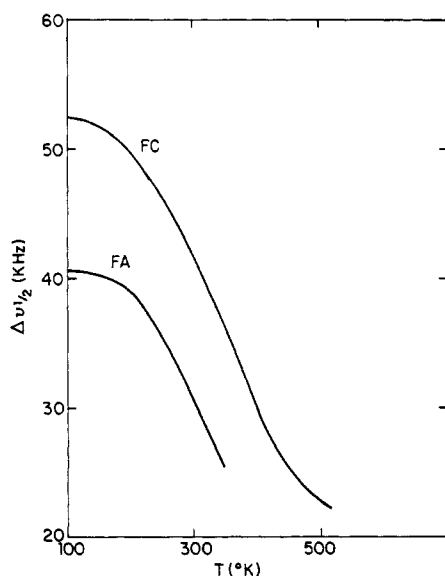


Figure 7. Proton NMR line width as a function of temperature for amorphous film (FA) and semicrystalline film (FC) of poly(ethylene terephthalate).

Proton NMR: Fiber and Film Samples. ^1H NMR spectra of semicrystalline fiber and film samples were recorded over the temperature range -170 to $+230$ $^{\circ}\text{C}$; amorphous fiber and film samples were restricted to the range -170 to $+70$ $^{\circ}\text{C}$ to avoid the risk of partial crystallization. As was seen for the powdered samples, the line shapes of both the semicrystalline and amorphous samples are composed mainly of a broad featureless component whose temperature dependence is illustrated in Figures 6 and 7 and a narrower component that is most easily distinguished at elevated temperatures. Table II gives values of the relative contribution of the narrow line shape to the total line shape for all of the semicrystalline samples at 162 $^{\circ}\text{C}$; it appears that all of the semicrystalline samples contain $\sim 4 \pm 2\%$ narrow component at this temperature.

Spin-lattice relaxation times in the rotating frame were obtained for both the fibers and films and are shown in Figures 8 and 9, respectively. The relaxation times are associated with the broad component of the line shape, which accounts for more than 80% of the total intensity for each sample, both semicrystalline and amorphous. The

Table II
Relative Contribution of the Narrow Component of the ^1H NMR Line Shape of Semicrystalline Poly(ethylene terephthalate) at 162 $^{\circ}\text{C}$

sample	% narrow line
fully protonated, powder	3.8 ± 1.3
aromatic protons, powder	4.2 ± 1.2
methylene protons, powder	2.8 ± 1.3
film (FC)	5.9 ± 2.0
fiber (CY)	3.2 ± 1.7

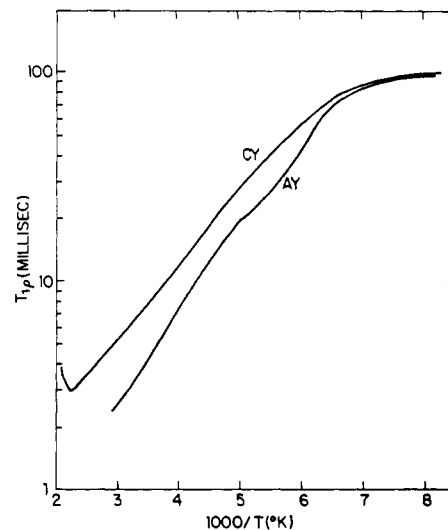


Figure 8. Proton spin-lattice relaxation times in the rotating frame as a function of temperature for amorphous yarn (AY) and semicrystalline yarn (CY) of poly(ethylene terephthalate).

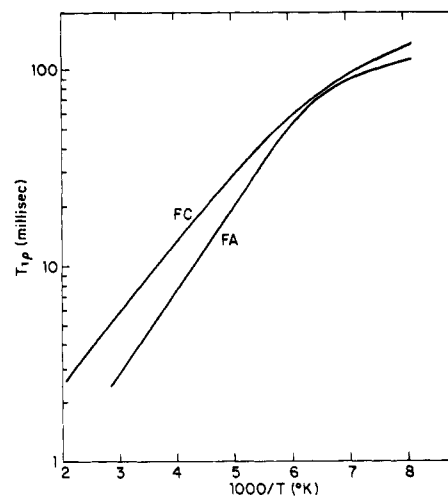


Figure 9. Proton spin-lattice relaxation time in the rotating frame ($\gamma(H_1) = 50$ kHz) as a function of temperature for amorphous film (FA) and semicrystalline film (FC) of poly(ethylene terephthalate).

relaxation behavior of amorphous specimens was singly exponential; however, the results reported for semicrystalline specimens are the long-time limiting slope, which ignores an apparent 10–30% component that relaxes more rapidly.

Spin-lattice relaxation times in the rotating frame ($\gamma(H_1) = 50$ kHz) were obtained for the narrow components of the proton line shapes in the frequency domain at those temperatures where they were readily detectable. Figure 10 illustrates $T_{1\rho}$ data as a function of temperature for a variety of semicrystalline fibers, films, and powdered samples. Data were collected only above ~ 400 K where sufficient signal was present to allow a precise delineation of the narrow component. These experiments were not

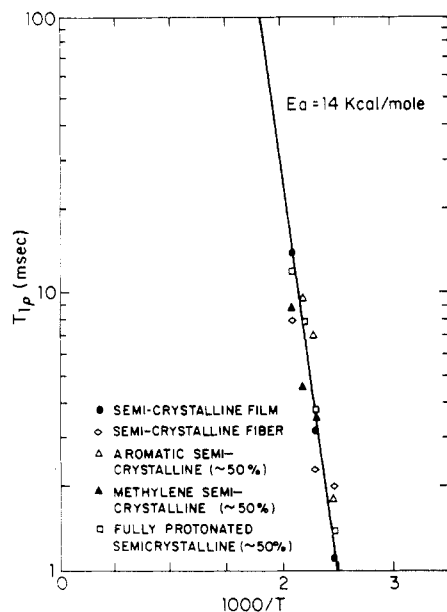


Figure 10. Proton spin-lattice relaxation time in the rotating frame ($\gamma(H_1) = 50$ kHz) as a function of temperature for the narrow component of the signal as a function of temperature for various semicrystalline poly(ethylene terephthalate) samples.

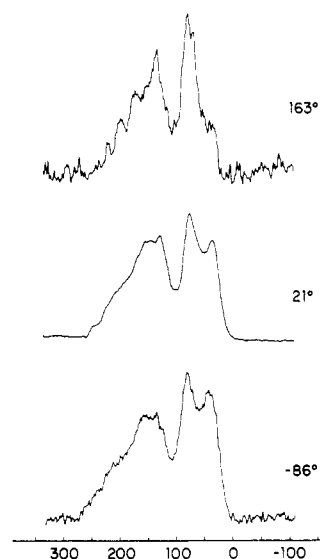


Figure 11. ^{13}C NMR powder pattern spectra (75.46 MHz) of initially amorphous poly(ethylene terephthalate) at temperatures between -86 and $+163^\circ\text{C}$. Some recrystallization has no doubt occurred in the 163°C spectrum. Horizontal scale is ppm with respect to external tetramethylsilane at $\delta = 0.0$ ppm.

carried out on amorphous samples due to extensive crystallization at these temperatures.

Carbon-13 NMR: Powdered Semicrystalline Poly(ethylene terephthalate). ^{13}C powder pattern spectra of fully protonated semicrystalline polymer were obtained over the range -100 to $+160^\circ\text{C}$. These spectra represent the superposition of powder patterns from at least four chemically distinct sites in the polymer, and Figures 11 and 12 illustrate the powder patterns observed for amorphous and semicrystalline material. The upfield (low frequency) portion of the spectrum is dominated by contributions from the methylene carbons, and the broader downfield (high frequency) portion of the spectrum has contributions from all aryl carbons and carboxyl carbons. The powder pattern observed over the temperature range -100 to $+30^\circ\text{C}$ changes very little, and previously reported¹⁰ shielding anisotropies calculated from room-tem-

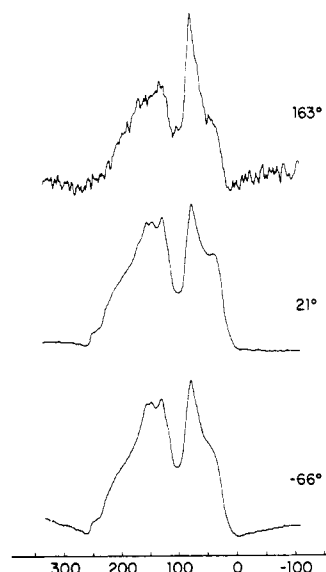


Figure 12. ^{13}C NMR powder pattern spectra (75.46 MHz) of semicrystalline poly(ethylene terephthalate) at temperatures between -66 and $+166^\circ\text{C}$. Horizontal scale is ppm with respect to external tetramethylsilane at $\delta = 0.0$ ppm.

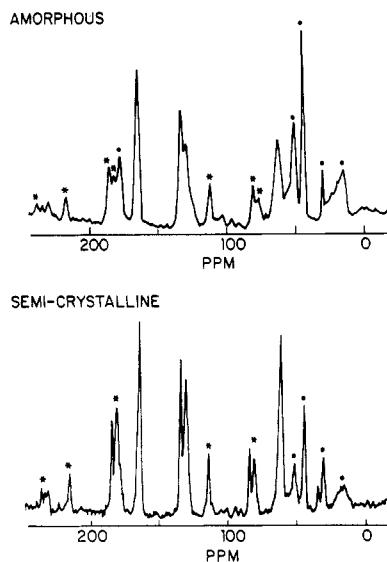


Figure 13. ^{13}C 75.46-MHz magic angle spinning spectra of amorphous and semicrystalline poly(ethylene terephthalate) obtained at room temperature with a spinning speed of 3.97 kHz, a cross-polarization time of 5 ms, and a decoupling/cross-polarization radio-frequency field strength of 64 kHz.

perature data should be a reasonably accurate representation of the motionally static values. The feature on the methylene line shape at ~ 50 ppm is of unknown origin. Attempts to acquire spectra of aliphatic and aromatic carbons separately via the use of selectively deuterated samples were frustrated by the very large loss of sensitivity observed in transient cross-polarization experiments.

Figure 13 illustrates ^{13}C magic angle spinning spectra acquired at 75.46 MHz with a cross-polarization time of 5 ms, radio-frequency field strengths of 64 kHz, and 3.97-kHz magic angle spinning. The spectra are cluttered with unwanted spinning sidebands that cause not only a loss in resolving power but also a significant loss in signal/noise in the isotropic resonances. Spectral lines marked with an asterisk are spinning sidebands and those marked with a dot are due to signals from the nominally perdeuterated poly(methyl methacrylate) rotor. It is obvious that the completely amorphous polymer has much

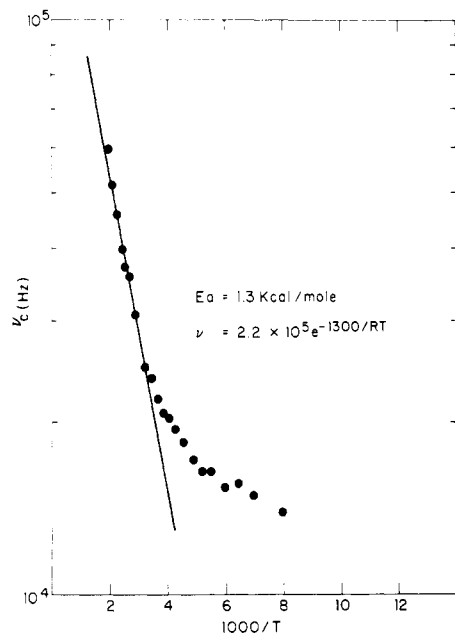


Figure 14. Conventional analysis (BPP) of temperature dependence of dipolar line narrowing data for powdered semicrystalline PET. The apparent activation energy and rate equation are given in the figure.

broader lines and a poorer signal/noise, even though both spectra were acquired with identical signal generation and averaging procedures. The broader lines in the spectrum of the amorphous polymer as compared to the semicrystalline polymer are due to a larger distribution of isotropic chemical shifts. The presence of broader lines in the spectrum of the amorphous polymer accounts for only part of the loss of signal/noise as compared to the semicrystalline polymer spectrum where the rotor background can be used as a standard; therefore, the signal generation method used here gives a distorted representation (half of the amorphous contribution to the line shape is observed)²¹ of the relative amorphous and crystalline populations in both the magic angle spinning and static spectra.

Discussion

The importance of considering the effects that both the amplitude and the rate of macromolecular motion play in the interpretation of magnetic resonance phenomena has been known for some time¹² but generally appreciated only recently. Examples include polyethylene,¹³ poly(tetrafluoroethylene) and its copolymers,¹⁴ poly(methyl methacrylate),¹⁵ polystyrene,¹⁶ and polybutadiene.¹⁷ In the following discussion of the experimental results for PET, we consider the amplitude as well as the rate of the motion of the polymer in each domain. The domain model used is qualitatively the same as that of Eichhoff and Zachmann^{4b} and involves three domains—crystalline, more mobile amorphous (MMA), and less mobile amorphous (LMA).

Proton NMR: Powdered Semicrystalline PET. The proton dipolar line shape over most of the temperature range examined is composed of at least two easily identified components—a broad and a narrow component. The broad component accounts for the majority of the spectral intensity at nearly all temperatures and is discussed first. The temperature dependence of the line width of the broad component for fully protonated and both partially deuterated polymers (Figure 2) illustrates that the rate at which the line width changes with temperature is nearly the same for both parts (methylene and aromatic) of the polymer; the difference in the static dipolar line widths

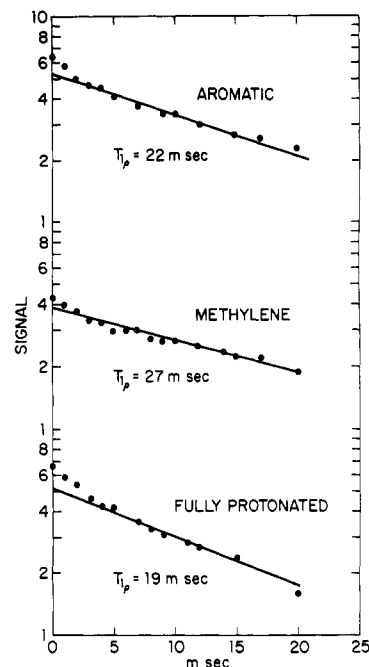


Figure 15. Spin-lattice relaxation in the rotating frame data for powdered semicrystalline PET at $\gamma(H_1) = 50$ kHz at room temperature.

for the methylene and aromatic groups simply reflects the closer proximity of other protons for the methylene as compared to the aromatic protons. These data could be subjected to a conventional analysis¹⁸ to extract an apparent rate and activation energy and would give the results illustrated in Figure 14. The use of this analysis implies that the rate of motion must be larger than, or comparable to, the strength of the dipolar interaction (~ 50 kHz) at the temperature (ca. -170°C) at which line narrowing is first observed. (Additionally, the deviation of the low-temperature line narrowing data from the simplest conventional model would be attributed to a distribution of processes with a corresponding distribution of correlation times and activation energies.) If the rate of motion were near 50 kHz at ca. -170°C , one would expect to see at least a local $T_{1\rho}$ minimum near this temperature. Examination of Figure 5 shows no $T_{1\rho}$ minimum for any sample below $+100^\circ\text{C}$; therefore, the observed line narrowing cannot be described by a model invoking only variation of rate(s) with temperature, and the temperature dependence of the angular amplitude of the motion must be considered as well.

Spin-lattice relaxation measurements carried out in both the rotating frame ($\gamma(H_1) = 50$ kHz) and the Zeeman frame ($\gamma(H_0) = 90$ MHz) may be used to qualitatively characterize the temporal nature of the motions extant over the temperature range examined. The $T_{1\rho}$ data reported in Figure 5 are the long-time limiting slope of the relaxation data. Actual data shown in Figure 15 illustrate that the nonexponential behavior of the $T_{1\rho}$ data is due to motional heterogeneity (e.g., crystalline or amorphous environment) in both the methylene and aromatic groups and is not due simply to inefficient spin diffusion between aromatic and methylene groups. The $T_{1\rho}$ experiment¹⁹ is most sensitive to motions near 100 kHz and relatively sensitive to those in the 10-kHz to 1-MHz range; if the motion present has significant spectral density in this frequency range at some temperature, a local $T_{1\rho}$ minimum will be observed. The absence of a $T_{1\rho}$ minimum below 100°C indicates that in the temperature range -170 to $+100^\circ\text{C}$, the rate of the motion(s) involved is either much less than 10 kHz or much

larger than 1 MHz. Previous reports^{20,21} of $T_{1\rho}$ measurements at room temperature for semicrystalline PET have reported deconvolution of the relaxation decays into a fast-relaxing component (55–65%) and a more slowly relaxing component (45–55%), where the former is attributed to amorphous regions and the latter to crystalline regions. However, the quantitative nature of this deconvolution seems doubtful since the crystallinity of these samples is thought to be near 50–60%, as measured by X-ray scattering for measuring crystallinity in PET. Indeed, more recent work has found that a variety of polyolefins as well as PET³⁷ are better described by a three-domain model with spin diffusion mixing the relaxation properties of each region to varying degrees. The $T_{1\rho}$ reported here for the broad component of the line shape indicate only an average relaxation rate for 70–80% of the sample and are heavily weighted with the slowest relaxing region (crystalline). Nevertheless, these results are quite adequate to locate the temperature at which significant spectral density exists in the 0.01–1-MHz range as indicated by a local $T_{1\rho}$ minimum. Spin-lattice relaxation data in the Zeeman frame as reported in Figure 4 are again for the broad component of the line shape and are singly exponential. These spin-lattice relaxation data are most sensitive to motions with a frequency of ~100 MHz and are reasonably sensitive to motions in the range 10 MHz to 1 GHz. The absence of any T_1 minimum below room temperature indicates that the motion(s) in this temperature regime must be characterized by rate(s) either much less than 10 MHz or much larger than 1 GHz. The T_1 data also reflect the efficiency of spin diffusion on this time scale via the observation of a single-exponential decay.²³ The dipolar line narrowing data, when examined in conjunction with the spin-lattice relaxation time measurements (T_1 , $T_{1\rho}$), indicate that the molecular motion(s) responsible for the observed narrowing are characterized by rates large compared to 1 GHz.

The motions responsible for the observed line narrowing behavior are rapid ($\gg 1$ GHz) at all temperatures below room temperature. These motions are obviously in the rapid-exchange or extreme-narrowing limit for all of the NMR measurements. A classical analysis^{18,19} of NMR relaxation behavior for this type of motion would predict that the relaxation times would become longer as the temperature is increased; this is the opposite of what is observed. The observed NMR behavior is due to a change in the amplitude of the motion with temperature rather than exclusively to a change in the rate of motion. The dependence of dipolar splittings in ordered systems upon amplitude of motion,²⁴ the dependence of relaxation rates^{25,26} for small molecules on the amplitude of restricted reorientation, and our previous work on the dependence of chemical shift¹⁴ and dipolar¹⁷ dominated line shapes provide a framework in which to describe the relationship between the amplitude of motion and the NMR phenomena.

Spatial averaging, or the amplitude of the motion, is reflected by that part of the second moment (M_2) that is modulated by the motion on the time scale of the measurement in question. Following Vega and Vaughan,²⁵ we can write the relation as

$$\Delta M_2 = M_2 - M_2(0) \quad (1)$$

where ΔM_2 is the fraction of the second moment that is modulated by the motion and $M_2(0)$ is the part of the second moment that is static on the time scale of the particular NMR experiment. The simplest form for the temperature dependence of the spatial averaging is

$$\Delta M_2 = M_2 e^{-\Delta E/RT} \quad (2)$$

where ΔE is the free energy necessary to allow the system to execute a larger degree of spatial averaging and is *not* an activation energy. (In a simplistic free energy vs. reaction coordinate diagram, ΔE is the difference of the zero-point energy of the two minima.) Spin-lattice relaxation rates (R) in both the Zeeman and rotating frame may be represented by

$$R \propto \Delta M_2 f(\tau_c) \quad (3)$$

where $f(\tau_c)$ is a spectral density function. If the motion responsible for the averaging is vibrational in nature ($\tau_c \lesssim 10$ ps) and may be modeled to first order as a harmonic oscillator, the vibrational correlation time will be independent of temperature. Therefore, it is the change in spatial averaging, as reflected in ΔM_2 , that is reflected in the narrowing of the dipolar line shapes and the relaxation behavior. A semiquantitative molecular interpretation of the temperature dependence of the spatial averaging is given below.

In addition to the motional averaging attributable to temperature-dependent spatial averaging, a second motional process is reflected in the $T_{1\rho}$ data for the methylene protons in Figure 5. A minimum in the $T_{1\rho}$ curve is observed at a temperature of $130 \pm 10^\circ\text{C}$. At the spin-locking field ($\gamma(H_1) = 50$ kHz) used, this corresponds to a correlation frequency of 100 kHz. Examination of Figure 1 indicates that this motion of the methylene group correlates with the previously observed α relaxation. Because the broad portion of the line shape contains contributions from both crystalline and less mobile amorphous regions (see below), the morphological identification of the α relaxation is not possible from these data alone. We note that a minimum is observed only in the methylene $T_{1\rho}$ data and, therefore, precludes this relaxation behavior as being due to cross-relaxation to the small amount of more mobile amorphous material (narrow line) that exhibits a much shorter $T_{1\rho}$ at these temperatures (see below). The molecular mechanics of the motion that the methylene groups undergo to give rise to the α relaxation cannot be definitively determined from the $T_{1\rho}$ data; however, in light of the restricted spatial averaging previously identified in both the aromatic and methylene moieties, it seems reasonable to postulate that the α relaxation is due to a very specific local motion of the methylene groups, possibly trans \leftrightarrow gauche isomerization. The temperature at which the $T_{1\rho}$ minimum appears is observed to be essentially independent of radio-frequency rotating field strength over the range $\gamma(H_1) = 30$ –70 kHz, thus indicating that this motion has a very large activation energy, which is consistent with the identification of this motion as the α relaxation.

A third distinct motional process is reflected in the spin-lattice relaxation times reported in Figure 4. A broad minimum in T_1 is observed for both the aromatic protons alone and the fully protonated polymer near room temperature. The methylene protons alone show essentially no perturbation to their relaxation behavior at this temperature. The minimum in the fully protonated polymer T_1 curve is less well-defined due to cross-relaxation between aromatic and aliphatic protons. This broad minimum corresponds to a frequency of 150 MHz at a reciprocal temperature of $3 \times 10^{-3} \text{ K}^{-1}$; comparison of this value to the relaxation plot of the β relaxation in Figure 1 indicates this feature correlates with the β relaxation. The β relaxation appears to be due to a local motion of the aromatic rings alone, not involving the methylene groups. One likely candidate for a specific molecular model of this

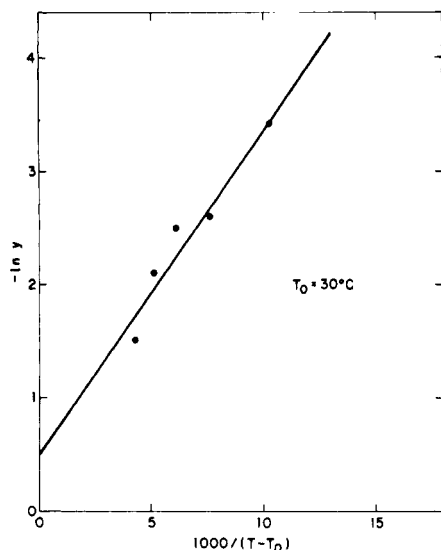


Figure 16. More mobile amorphous (MMA) fraction of PET as a function of inverse reduced temperature.

motion is aromatic ring flips. This molecular mechanism is consistent with the previous description of temperature-dependent spatial averaging being the predominant motion, if only a minor fraction of the polymer undergoes ring flipping at these temperatures. Spin diffusion from this fraction of the polymer to the remainder would give the observed single-exponential relaxation behavior. This fraction of the polymer is most likely less mobile amorphous (LMA; see below) and thus we may tentatively assign the β relaxation to a specific motion of the aromatic rings (perhaps ring flips) in a limited fraction of the polymer (probably LMA).

In addition to the broad component of the proton dipolar line shape, a narrower component is observed above -10°C , whose relative intensity increases with temperature as shown in Figure 3. The narrow component cannot be due to cyclic oligomers or other low molecular weight material as this material is known²⁷ to comprise less than 2% of commercial PET samples and we observe a much larger contribution than this at elevated temperatures (Figure 3). The origin of the narrow component has been ascribed^{4b,28} to more mobile amorphous (MMA) polymer, whereas the broad component is due to crystalline and less mobile amorphous (LMA) polymer. The MMA phase is thought to be domains where sufficient free volume exists to allow the amplitude of the motion to be large enough to yield a significantly larger amount of spatial averaging than takes place in either the crystalline or LMA regions. The amount of MMA material increases with temperature and this behavior can be analyzed by employing the free volume arguments of Eichhoff and Zachmann.^{4b} The fraction of total polymer that is MMA at any temperature is $y(T)$, the total amorphous content is y_0 , the critical value of free volume above which LMA becomes MMA is V_{fkr} , α is the average value of the thermal expansion coefficient, V_m is the volume per segment over the temperature range used, T_0 is the temperature at which MMA is first observed, and γ is an adjustable factor between 0.5 and 1.0.

$$y(T) = y_0 e^{-(\gamma V_{\text{fkr}}/(\alpha V_m(T-T_0)))} \quad (4)$$

Figure 16 illustrates the good agreement between the experimental data of Table I and this treatment. A least-squares fit of the data to eq 4 gives a value of 60% for total amorphous content and this value is quite close to that found in previous $T_{1\rho}$ deconvolutions,^{20,21} indicating once again the presence of spin diffusion as a complication. A

value for the relative critical free volume can be estimated (by using the thermal expansion coefficient²⁹ ($70^\circ\text{C} < T < 160^\circ\text{C}$) of $2.69 \times 10^{-4}^\circ\text{C}^{-1}$) to be $V_{\text{fkr}}/V_m = 0.08$. The value of the relative critical free volume is to be compared to that which may be calculated from a theoretical equation of state³⁰ using $T^* = 11710^{29}$ (T^* = characteristic temperature) and $T_g = 70^\circ\text{C}$ ²⁹ to yield a value of the excess free volume of 0.062. The qualitative success of the free volume model enables us to characterize the narrower component of the dipolar line shape as arising from amorphous regions of the polymer and the broader component as arising from both the crystalline regions and from the less mobile amorphous regions. More detailed descriptions²⁸ of the morphological origin of MMA and LMA have concluded that LMA is identified as taut tie molecules, and MMA is either loops or nontaut tie molecules. A classical analysis¹⁸ of the observed $T_{1\rho}$ data for the narrow component of the line shape (Figure 10), ignoring the temperature dependence of ΔM_2 , gives an apparent activation energy of 14 kcal/mol, which is in fortuitous agreement with the activation energy found for the β relaxation;¹ however, the rate of this motion over the observed temperature range is several orders of magnitude larger than that observed or extrapolated for the β relaxation over the same temperature range. The apparent activation energy characterizing the $T_{1\rho}$ relaxation reflects not only the temperature dependence of the rate of the motion but also the temperature dependence of the amplitude of the motion, and the $T_{1\rho}$ measurement alone cannot deconvolute the individual contributions.

Proton NMR: Film and Fiber PET. Comparison of the narrowing of the dipolar line shape observed for semicrystalline fibers (Figure 6), semicrystalline films (Figure 7), and semicrystalline fully protonated powdered polymer (Figure 2) illustrates the essentially identical behavior of these different forms of PET. The amorphous yarn and film have a smaller static line width, reflecting the larger amount of static disorder in a fully amorphous sample, but the rate at which this line width narrows with temperature is only very slightly larger than that of the semicrystalline polymer. This observation suggests that the dominant molecular process responsible for the narrowing of the broad component of the dipolar line shape with temperature is local chain dynamics, rather than large-scale cooperative motions which are enhanced by additional free volume. The question of the relationship between static and dynamic disorder is more fully addressed by the molecular model given in the following section.

The temperature dependence of $T_{1\rho}$ for the semicrystalline yarn and film (Figures 8 and 9) is qualitatively similar to that observed for the powdered semicrystalline polymer (Figure 5) since the relaxation time decreases monotonically with increasing temperature, until a minimum is observed at $\sim 140^\circ\text{C}$ for the semicrystalline yarn. The reason that a minimum is observed for the semicrystalline yarn and not for the semicrystalline film or powdered polymer is not known. Figure 17 illustrates the dilemma presented when attempting to extract a number of relaxation times from a $T_{1\rho}$ measurement. The behavior of the amorphous polymer is very nicely described by a single-exponential decay and the behavior of $\sim 90\%$ of the semicrystalline polymer appears to be well described by a longer single-exponential decay; however, the semicrystalline polymer does not have a component representing the amorphous material ($\sim 50\%$) with a relaxation time near that found for a fully amorphous polymer. This difficulty is due to the presence of substantial spin diffusion during the time of the relaxation measurement, thus

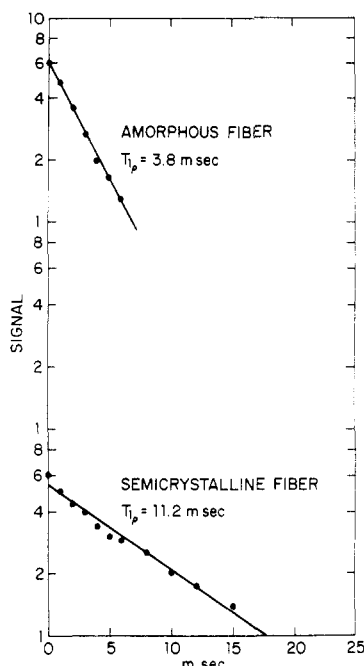


Figure 17. Residual magnetization as a function of spin-locking time in a $T_{1\rho}$ measurement ($\gamma(H_1) = 50$ kHz) of amorphous and semicrystalline PET fiber.

making simple biexponential fitting a meaningless procedure for the extraction of either the relative amounts of each component or their relaxation rates. Spin diffusion may be suppressed with the use of multiple-pulse techniques and a relaxation time in the interaction frame, which is quite similar to a $T_{1\rho}$ measurement, can give useful information in a polymeric system.¹⁴ A previous attempt²⁰ to use multiple-pulse methods to measure relaxation times in PET met with mixed results. We have been unsuccessful in employing multiple-pulse methods on PET due to radio-frequency pulse instabilities over the time scale necessary to characterize the relaxations (≈ 50 ms). $T_{1\rho}$ results for the amorphous yarn and film indicate that a qualitatively similar motion must be responsible for the relaxation behavior in both of these forms of the polymer. The shorter values of the relaxation times and the slightly larger rate of decrease in relaxation time with increasing temperature for the amorphous polymer both reflect the somewhat larger amount of spatial averaging that occurs in the glassy state.

¹³C NMR: Semicrystalline Powdered PET. Variable-temperature static (nonspinning) ¹³C spectra obtained with dipolar decoupling (Figures 11 and 12) are powder pattern ¹³C chemical shift line shapes. Previous work³¹ has demonstrated that chemical shift line shapes are sensitive to reorientational motions in polyesters at frequencies near 10 kHz, making these measurements an alternative to ¹³C $T_{1\rho}$ measurements, which are themselves often inconclusive due to spin dynamics complications.³² The lowest temperature nonspinning ¹³C spectra for both amorphous and semicrystalline PET must be very near the slow-motion limit, as indicated by the proton dipolar line width at these temperatures (Figure 2); the highest temperature spectra correspond to the temperature at which the ¹H dipolar line shape has been narrowed by $\sim 40\%$. The absence of a large amount of narrowing in the ¹³C spectra indicates that some of the observed narrowing of the proton dipolar line shape must be due to averaging of intermolecular contributions to M_2 which are more sensitive to both translational motions³³ and to small-angle librations (especially the aromatic groups) than are the intramolecular contri-

butions. Careful examination of the temperature dependence of the upfield (mainly methylene line shape) and downfield (aromatic and carbonyl) portions of the line shapes does reveal somewhat more motional narrowing in the upfield portion of the line shape. This observation would indicate that the rate or amplitude of the methylene motion is larger than that of the aromatic moiety. Line shape changes of $\leq 10\%$ correspond to librational motions of $\leq \pm 20^\circ$ and are at the limit of detectability. The temperature dependence of the chemical shift line shape adds considerably to our description of the molecular motion when considered in conjunction with the proton NMR results; i.e., the predominant motion in PET is one in which the amplitude of a very rapid motion(s) grows with temperature and this motion is largest for the methylene moieties and must be $\geq \pm 20^\circ$ above 160°C . We note again that these conclusions are shown by the magic angle spinning results to reflect both the amorphous and crystalline portions of the polymer; however, the amorphous contribution to the spectra is underestimated by a factor of 2.²¹

Molecular Model of Temperature-Dependent Spatial Averaging. Temperature-dependent spatial averaging may be phenomenologically described by eq 1–3 for the case of a dipolar line shape of a randomly oriented sample. This model may be related to the amplitude of the molecular motion by consideration of the mechanics of the motion. The reorientational motions that occur far below 120°C , which are somewhat larger for the methylene groups than for the aryl groups, are not large fluctuations such as *trans* \leftrightarrow *gauche* isomerizations or ring flips due to the small and gradual decreases in the line width. Therefore, these motions must be small-amplitude librations. The amplitude of the libration grows with temperature, thus modulating a larger fraction of M_2 as the temperature increases. The rigid lattice second moment of the dipolar line shape is related to the geometry of the nuclear spins via eq 5, where K is a constant, r_{ij} is the internuclear separation between spin pairs, and θ_{ij} is the angle that r_{ij} makes with the static magnetic field (H_0).

$$M_2 = K \sum_{i \neq j} (3 \cos^2 \theta_{ij} - 1)^2 / r_{ij}^6 \quad (5)$$

Small-angle librations will cause M_2 to be modulated only via fluctuations in θ_{ij} , if only intramolecular contributions to M_2 are considered. Then we have

$$M_2 = K \sum_{i \neq j} \frac{(3 \cos^2 \theta_{ij} - 1)^2}{r_{ij}^6}$$

If the symmetry of the small-angle libration is such that the molecular interaction vector \vec{r} (see Figure 18) samples orientations which have an axially symmetric distribution about a direction, d , then

$$\langle 3 \cos^2 \theta_{ij} - 1 \rangle = \frac{1}{2} \langle 3 \cos^2 \beta - 1 \rangle \langle 3 \cos^2 \alpha - 1 \rangle \quad (6)$$

where α is the angle between H_0 and d , β is the angle between d and r , and S_β is an order parameter and is defined as

$$S_\beta = \frac{1}{2} \langle 3 \cos^2 \beta - 1 \rangle \quad (7)$$

where S_β is experimentally defined from eq 1 as

$$S_\beta^2 = M_2(0) / M_2 \quad (8)$$

In this idealized case, S_β may be related to an average value of β ; however, the amplitude of motion is not expected to be the same for all parts of the chain and can be described by a distribution of amplitudes. If the probability distribution is random, a Gaussian distribution may be used

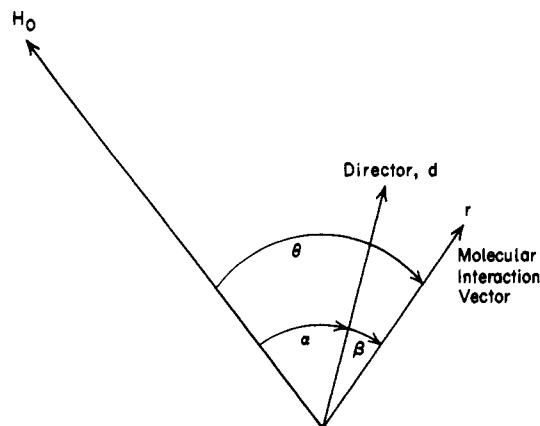


Figure 18. Coordinate system describing the relationship between the static magnetic field (H_0), the molecular interaction vector (\vec{r}), and the average position of \vec{r} or the local director (\vec{d}). \vec{H}_0 is the direction of the applied magnetic field. The director, \vec{d} , is the average orientation of the molecular interaction vector \vec{r} . All values of θ are possible in an unoriented sample. The angle β is a measure of the deviation of the molecular interaction vector from its average position. The molecular interaction vector is the vector between any two protons on the same chain and is synonymous in this case with the internuclear vector.

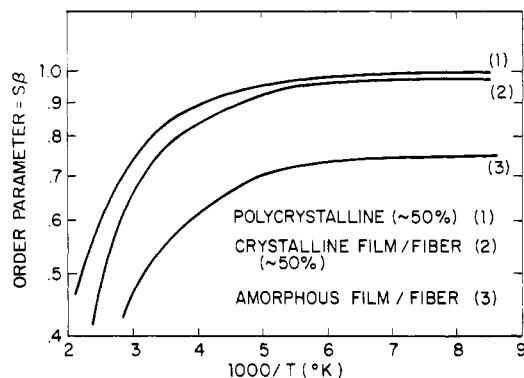


Figure 19. Proton dipolar order parameter, disregarding translational motion corrections, for various forms of PET as a function of temperature.

to describe it with a standard deviation of β_0 . β_0 is defined by eq 9.

$$S_\beta = \frac{1}{2} \frac{\int_0^\pi (3 \cos^2 \beta - 1) e^{-(1/2)(\beta/\beta_0)^2} \sin \beta \, d\beta}{\int_0^\pi e^{-(1/2)(\beta/\beta_0)^2} \sin \beta \, d\beta} \quad (9)$$

Analysis of dipolar line width data following eq 8 for semicrystalline powder, film, and fiber and amorphous film and fiber is given in Figure 19. This analysis ignores the intermolecular contribution^{4a} (~20%) to M_2 and the greater ease of orientational averaging of this fraction of M_2 . Averaging of the intermolecular contribution could account for 30% of the observed dipolar line narrowing and, thus, the calculated S_β is a lower limit. Smaller order parameters for amorphous PET at all temperatures are due mainly to static disorder; dynamic disorder is more accurately reflected by (dS_β/dT) for any form of the polymer. Figure 20 illustrates the standard deviation of a Gaussian distribution (β_0) of small-angle vibrations for amorphous and semicrystalline PET. The values given in Figure 20 are an upper limit and are an average over the methylene and aromatic groups for the fully amorphous polymer; additionally, the values for the semicrystalline polymer are an average over LMA and crystalline regions. Nevertheless, this analysis indicates that the average amplitude of motion in the amorphous regions is somewhat

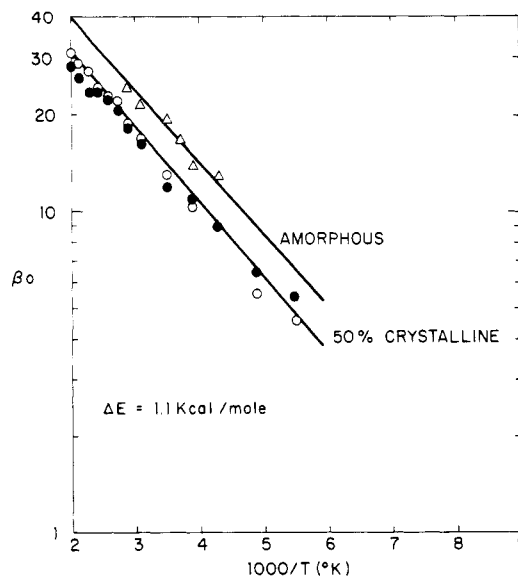


Figure 20. Upper limit for one standard deviation of a Gaussian distribution of small-angle vibrations for amorphous and semicrystalline PET as a function of temperature. The open circles are methylene groups alone, the filled circles are aromatic groups alone, and the open triangles are fully protonated polymer.

larger than in the crystalline portions of the polymer and the values of β_0 at 160 °C ($\beta_0 \lesssim 35^\circ$ amorphous; $\beta_0 \lesssim 20^\circ$ crystalline) are not in conflict with those estimated from ^{13}C chemical shift line shapes ($\beta_0 \gtrsim 20^\circ$ for methylene groups). The amplitude of motion in both the crystalline and amorphous regions grows at the same rate and is characterized by a free energy $\Delta E = 1.1$ kcal/mol.

Summary and Conclusions

The semiquantitative model of chain motion in PET that has been developed here requires the use of three distinct environments, each of which is characterized by both a rate and amplitude of motion.

1. Motion in the crystalline regions of the polymer is dominated by rapid ($\tau_c \ll 10^{-9}$ s) relatively small angular fluctuations that grow with increasing temperature. At 160 °C the "average" amplitude of the methylene angular fluctuations is $\sim 20^\circ$ and the amplitude of the aromatic fluctuations is smaller and is less than 20° .

2. Motion in the less mobile amorphous regions is also dominated by rapid relatively small angular fluctuations that increase in amplitude with increasing temperature. The amplitudes are somewhat larger than those in the crystalline regions at all temperatures. The amplitude of the methylene reorientation is once again greater than that of the aromatic group and is estimated by extrapolation to be in the range $20\text{--}35^\circ$ at 160 °C, whereas the aromatic ring fluctuations are smaller and are less than 20° . The amplitude of motion of both methylene and aromatic groups in both the crystalline and less mobile amorphous regions grows with a temperature dependence characterized by a free energy of 1.1 kcal/mol.

3. Methylene groups in the crystalline and/or less mobile amorphous regions execute a unique motion (perhaps $\text{trans} \leftrightarrow \text{gauche}$ isomerization) that is characterized by a rate of 100 kHz at 130 ± 10 °C and a very high activation energy which correlates with the α relaxation.

4. Aromatic groups undergo a unique motion (perhaps ring flips) in a limited portion of the polymer (probably LMA) at a rate of ~ 150 MHz near 50 °C. This motion correlates with the β relaxation.

5. The fraction of amorphous material that may be characterized as more mobile amorphous grows with tem-

perature and is related to the free volume available to permit increased spatial averaging. At 160 °C, somewhat less than 50% of the amorphous material is more mobile amorphous and the rate of motion of both the methylene and aromatic groups is much larger than 100 kHz and the amplitude is larger than that present in the less mobile amorphous regions.

Rapid angular fluctuations have been found previously to be a significant mode of motion not only in synthetic polymers¹³⁻¹⁷ but in biological systems³⁴ as well. A more direct confirmation of the details of this model of motion for PET is available from temperature-dependent ²H NMR line shape analysis^{15,35} which gives quantitative values for the magnitude of angular fluctuations of both methylene and aromatic groups in the crystalline domains that are in agreement with the range of values given by the present model. The present model illustrates the inherent difficulty in defining either the rate or the amplitude of the motion with only a single measurement, and this dilemma has indeed been demonstrated for PET with ¹³C *T*_{1ρ} measurements.³⁶ Rapid angular fluctuations would be observed in dielectric or anelastic measurements as a growth of the strength of a tan δ peak with temperature at essentially constant frequency; however, the frequency of these angular fluctuations is much too large to be detected by either mechanical or dielectric measurement and these motions are therefore transparent to either mechanical or dielectric probes.

Acknowledgment. We gratefully acknowledge Dr. F. P. Gay (Polymer Products Department, E. I. du Pont de Nemours and Company) for preparation of the partially deuterated polymers, Drs. R. M. Ikeda, H. W. Starkweather, C. J. Heffelfinger, and A. J. Vega and Professor R. Simha for stimulating discussions, Professor K. J. Packer for a critical reading of the manuscript, and Mr. R. O. Balback for skilled technical assistance.

Registry No. PET (SRU), 25038-59-9.

References and Notes

- (1) N. G. McCrum, B. E. Read, and G. Williams, "Anelastic and Dielectric Effects in Polymeric Solids", Wiley, New York, 1967.
- (2) (a) R. L. Land, R. E. Richards, and I. M. Ward, *Trans. Faraday Soc.*, **55**, 225 (1959). (b) I. M. Ward, *J. Chem. Phys.*, **31**, 858 (1959). (c) I. M. Ward, *Trans. Faraday Soc.*, **56**, 648 (1960). (d) G. Farrow and I. M. Ward, *Br. J. Appl. Phys.*, **11**, 543 (1960). (e) G. Farrow, J. McIntosh, and I. M. Ward, *Makromol. Chem.*, **38**, 147 (1960). (f) A. Cunningham, A. J. Manuel, and I. M. Ward, *Polymer*, **17**, 125 (1976). (g) I. M. Ward, "Mechanical Properties of Solid Polymers", Wiley, New York, 1971, pp 180-181.
- (3) T. M. Connor, *Trans. Faraday Soc.*, **60**, 1574 (1963).
- (4) (a) U. Eichhoff and H. G. Zachmann, *Phys. Status Solidi A*, **1**, K127 (1970). (b) U. Eichhoff and H. G. Zachmann, *Ber. Bunsenges. Phys. Chem.*, **74**, 919 (1970). (c) U. Eichhoff and H. G. Zachmann, *Kolloid Z. Z. Polym.*, **241**, 928 (1970).
- (5) R. P. Daubeney, C. W. Bunn, and C. J. Brown, *Proc. R. Soc. London, Ser. A*, **226**, 531 (1954).
- (6) S. R. Hartmann and E. L. Hahn, *Phys. Rev.*, **128**, 2042 (1962).
- (7) A. R. Sharp and M. M. Pintar, *Proc. XVI Colloq. AMPERE (Bucharest)* 1970.
- (8) ASTM Method D1505. Limiting densities are $\rho_a = 1.33 \text{ g/cm}^3$ and $\rho_c = 1.455 \text{ g/cm}^3$. Powdered samples were prepared by cryogenically grinding melt-polymerized polymer.
- (9) L. B. Schreiber and R. W. Vaughan, *J. Catal.*, **40**, 226 (1975).
- (10) P. DuBois Murphy, T. Taki, B. C. Gerstein, P. M. Henrichs, and D. J. Massa, *J. Magn. Reson.*, **49**, 99 (1982).
- (11) J. S. Frye and G. E. Maciel, *J. Magn. Reson.*, **48**, 125 (1982).
- (12) D. W. McCall and E. W. Anderson, *J. Polym. Sci., Part A*, **1**, 1175 (1963).
- (13) J. Collignon, H. Sillescu, and H. W. Spiess, *Colloid Polym. Sci.*, **259**, 220 (1981).
- (14) A. J. Vega and A. D. English, *Macromolecules*, **13**, 1635 (1980).
- (15) A. J. Vega, *Polym. Prepr., Am. Chem. Soc., Div. Polym. Chem.*, **22**, 282 (1981).
- (16) H. W. Spiess, *Colloid Polym. Sci.*, **261**, 193 (1983).
- (17) (a) A. D. English and C. R. Dybowski, *Macromolecules*, **17**, 446 (1984). (b) A. D. English, *Macromolecules*, submitted.
- (18) H. S. Gutowsky and G. E. Pake, *J. Chem. Phys.*, **18**, 162 (1950).
- (19) V. J. McBrierty, *Polymer*, **15**, 503 (1974).
- (20) T. T.-P. Cheung, B. C. Gerstein, L. M. Ryan, R. E. Taylor, and C. R. Dybowski, *J. Chem. Phys.*, **73**, 6059 (1980).
- (21) R. S. Aujila, R. K. Harris, K. J. Packer, M. Parameswaran, and B. J. Say, *Polym. Bull.*, **8**, 253 (1982).
- (22) K. J. Packer, J. M. Pope, R. R. Yeung, and M. E. A. Cudby, *J. Polym. Sci., Polym. Phys. Ed.*, **22**, 589 (1984).
- (23) The ordering of the relaxation times (*T*₁, *T*_{1ρ}) for aromatic > methylene > fully protonated polymer is indicative of not only the magnitude of the dipolar interaction that is modulated (fully protonated > methylene > aromatic) but that intermolecular contributions to the dipolar interaction are small.
- (24) N. O. Petersen, Ph.D. Thesis, California Institute of Technology, 1977.
- (25) A. J. Vega and R. W. Vaughan, *J. Chem. Phys.*, **68**, 1958 (1978).
- (26) M. Polak and D. C. Ailion, *J. Chem. Phys.*, **67**, 3029 (1977).
- (27) I. Goodman and B. F. Nesbitt, *J. Polym. Sci.*, **48**, 423 (1960).
- (28) H. G. Zachmann, *Polym. Eng. Sci.*, **19**, 966 (1979).
- (29) P. Zoller and P. Bolli, *J. Macromol. Sci., Phys.*, **B18** (3), 555 (1980).
- (30) R. Simha and P. S. Wilson, *Macromolecules*, **6**, 908 (1973).
- (31) P. Sergot, F. Laupretre, C. Louis, and J. Virlet, *Polymer*, **22**, 1150 (1981).
- (32) D. L. VanderHart, *J. Chem. Phys.*, **71**, 2773 (1979).
- (33) S. J. Opella and J. S. Waugh, *J. Chem. Phys.*, **66**, 4919 (1977).
- (34) T. A. Cross and S. J. Opella, *J. Mol. Biol.*, **159**, 543 (1982).
- (35) A. J. Vega, unpublished results.
- (36) M. D. Sefcik, J. Schaefer, E. O. Stejskal, and R. A. McKay, *Macromolecules*, **13**, 1132 (1980).
- (37) D. L. VanderHart and J. R. Havens, *26th Rocky Mountain Conf. Proc.*, 127 (1984).